

Unsaturated both large positive and negative magnetoresistance in Weyl Semimetal TaP

Jianhua Du,¹ Hangdong Wang,² Qianhui Mao,¹ Rajwali Khan,¹ Binjie Xu,¹ Yuxing Zhou,¹ Yannan Zhang,¹ Jinhua Yang,² Bin Chen,² Chunmu Feng,¹ and Minghu Fang^{1,3,*}

¹*Department of Physics, Zhejiang University, Hangzhou 310027, China*

²*Department of Physics, Hangzhou Normal University, Hangzhou 310036, China*

³*Collaborative Innovation Center of Advanced Microstructures, Nanjing 210093, China*

(Dated: March 5, 2022)

After growing successfully TaP single crystal, we measured its longitudinal resistivity (ρ_{xx}) and Hall resistivity (ρ_{yx}) at magnetic fields up to 9T in the temperature range of 2-300K. It was found that at 2K its magnetoresistivity (MR) reaches to $3.28 \times 10^5\%$, at 300K to 176% at 8T, and both do not appear saturation. We confirmed that TaP is indeed a low carrier concentration, hole-electron compensated semimetal, with a high mobility of hole $\mu_h = 3.71 \times 10^5 \text{ cm}^2/\text{V s}$, and found that a magnetic-field-induced metal-insulator transition occurs at room temperature. Remarkably, as a magnetic field (H) is applied in parallel to the electric field (E), the negative MR due to chiral anomaly is observed, and reaches to -3000% at 9T without any signature of saturation, too, which distinguishes with other Weyl semimetals (WSMs). The analysis on the Shubnikov-de Haas (SdH) oscillations superimposing on the MR reveals that a nontrivial Berry's phase with strong offset of 0.3958 realizes in TaP, which is the characteristic feature of the charge carriers enclosing a Weyl nodes. These results indicate that TaP is a promising candidate not only for revealing fundamental physics of the WSM state but also for some novel applications.

PACS numbers: 72.90+y;72.10.-d;72.15.Om

The Weyl semimetal (WSM) phase, in which the bulk electronic bands disperse linearly along all momentum direction through a node, the Weyl point, in a three-dimension (3D) analogue of graphere, can be viewed as an intermediate phase between a trivial insulator and a topological insulator[1–5]. Although a number of candidates for a WSM were previously proposed, such as, $\text{Y}_2\text{Ir}_2\text{O}_7$ [6] and HgCr_2Se_4 [7] compounds, in which magnetic order breaks the time-reversal symmetry, and $\text{LaBi}_{1-x}\text{Sb}_x\text{Te}_3$ [8] compound, in which fine-tuning the chemical composition is necessary for breaking inversion symmetry, a WSM has not realized experimentally in any of these compounds due to either no enough large magnetic domain or difficulty to tune the chemical composition within 5%. Very recently, the theoretical proposal[9, 10] for a WSM in a class of stoichiometric materials, including TaAs, TaP, NbAs and NbP, which break crystalline inversion symmetry, has been soon confirmed by the experiments[11–14], except for TaP due to difficulty to grow large crystal. The exotic transport properties exhibiting in these materials ignite an extensive interesting in both the condensed matter physics and material science community, especial for their extremely large magnetoresistance (MR) and ultrahigh mobility of charge carriers.

Materials with large MR have been used as magnetic sensors[16], in magnetic memory[17], and in hard drives[18] at room temperature. Large MR is an uncommon property, mostly of magnetic compounds, such as a giant magnetoresistance (GMR)[19] emerging in Fe/Cr thin-film, and colossal magnetoresistance (CMR) in the

manganese based perovskites[20, 21]. In contrast, ordinary MR, a relatively weak effect, is commonly found in non-magnetic compounds and elements[22]. Magnetic materials typically have negative MR. Positive MR is seen in metals, usually at the level of a few percent, and in some semiconductors, such as 200% at room temperature in $\text{Ag}_{2+\delta}(\text{Te,Se})$ [30], comparable with those of materials showing CMR[24], and semimetals, such as high-purity bismuth, graphite[25], and $4.5 \times 10^4\%$ in WTe_2 [26]. In the semimetals, very high MR is attributed to a balanced hole-electron "resonance" condition, as described in Ref.[26]. WSM provides another possibility to realize extremely large MR, as observed in TaAs[13, 14], NaAs[27] and NbP[12], moreover, the helical Weyl fermions with unprecedented mobility are well protected from defect scattering by real spin conservation associated to the chiral Weyl nodes. Thus, it is very interesting not only for fundamental physics, but also for practical application to search for more WSM compounds and characterize their MR behavior.

TaP crystalizes in a body-centered tetragonal lattice with nonsymmorphic space group $I4_1md(No.109)$, which lacks inversion symmetry, shown in Fig. 1(a), which is one of the member predicted as a WSM in Refs.[9, 10]. In this letter, we grew successfully TaP single crystal, then measured its longitudinal resistivity (ρ_{xx}) and Hall resistivity (ρ_{yx}) at magnetic fields up to 9T and in the temperature range of 2-300K. It is found that at 2K its MR reaches to $3.28 \times 10^5\%$, and at 300K to 176% at 8T, and both do not appear saturation, and a magnetic-field-induced metal-insulator transition occurs at room

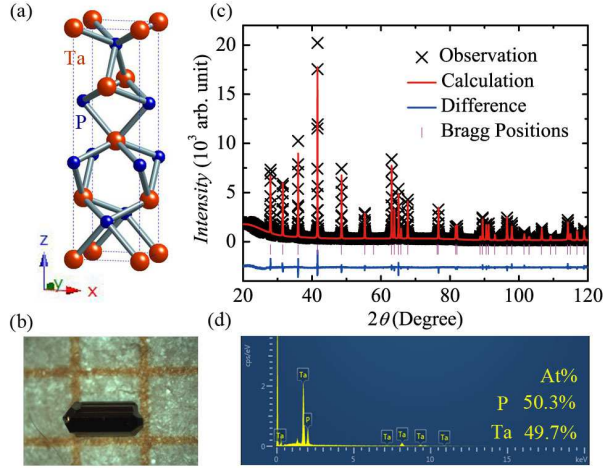


FIG. 1. (Color online) (a) Crystal structure of TaP with a body-centered tetragonal structure. (b) Photo of TaP crystal. (c) XRD pattern of powder obtained by grinding TaP crystals. Its Rietveld refinement is shown by the line. (d) Energy Dispersive X-ray Spectrometer (EDXS) for the TaP crystal.

temperature. Hall resistivity measurements confirmed that TaP is indeed a low carrier concentration, hole-electron compensated semimetal, with the high mobility $\mu_h = 3.71 \times 10^5 \text{ cm}^2/\text{V s}$. Remarkably, as a magnetic field (H) is applied in parallel to the electric field (E), the negative MR due to chiral anomaly is observed, reaches to near -3000% at 9T without any signature of saturation, which distinguishes with other WSMs and may originate from a larger distance between Weyl nodes in the momentum space. We have also confirmed that a nontrivial Berry's phase with strong offset of 0.3958 realizes in TaP, which is the characteristic feature of the charge carriers enclosing a Weyl nodes.

Single crystals of TaP were grown using a chemical vapor transport method. Polycrystalline TaP prepared previously was filled in the quartz tube with a $10\text{mg}/\text{cm}^3$ Iodine as a transporting agent. After evacuated and sealed, the quartz tube was heated for three weeks in a tube furnace with a temperature field of $\Delta T = 950\text{--}850^\circ\text{C}$. Large polyhedral crystals with dimensions up to 1.0 mm were obtained, as shown in Fig. 1(b). Energy Dispersive X-ray Spectrometer (EDXS) was used to determine the crystal composition, and stoichiometric TaP was confirmed. X-ray diffraction (XRD) pattern [see Fig. 1(c)] at room temperature of the TaP powder by grinding pieces of crystals confirms its tetragonal structure, and its Rietveld refinement (reliability factor: $R_{wp} = 7.18\%$, $\chi^2 = 2.973$) gives the lattice parameters of $a = 3.3184(\pm 0.0001) \text{ \AA}$ and $c = 11.3388(\pm 0.0001) \text{ \AA}$. Electrical resistivity in magnetic field (H) and Hall resistivity measurements were carried out using a Quantum Design Physical Property Measurement System (PPMS).

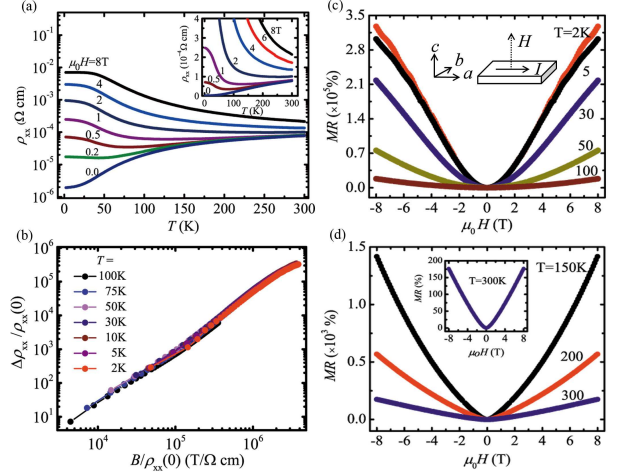


FIG. 2. (Color online) (a) Temperature dependence of longitudinal resistivity, $\rho_{xx}(T)$, measured at different magnetic field for TaP single crystal. (b) MR scaling law with magnetic field (c) Magnetic field dependence of MR for below 100K. (d) for above 100K.

Figure 2 summarizes the resistivity (ρ_{xx}) results measured at different H , which was applied in c axis, and normal to the current, and various temperatures (T) of TaP crystal. As shown in Fig. 2(a), the temperature dependence of resistivity, $\rho_{xx}(T)$, at $H=0\text{T}$ displays a metallic behavior with $\rho(300\text{K}) = 77.98 \mu\Omega \text{ cm}$, and $\rho(2\text{K}) = 1.933 \mu\Omega \text{ cm}$, thus estimated residual resistivity ratio [RRR] = $\rho(300\text{K})/\rho(2\text{K}) \sim 40$. It is obvious that the crossover from "metallic" to "insulating" behavior as a magnetic field is applied, that looks like a magnetic-field-induced metal-insulator transition. On lowering the temperature the resistivity increases, as it does in an insulator, but then saturates towards field-dependent constant values at the lowest temperature, more clearly seen in the log-log plot in the main panel of Fig. 2(a). The similar behavior has also been observed in the conventional semimetals, such as high-purity Bi[22], graphite[28, 29], WTe_2 [26] and $\beta\text{-Ag}_2\text{Te}$ [30, 31], and in the Dirac semimetal Cd_3As_2 [32] and other Weyl semimetals TaAs[10, 14], NbAs[33] and NbP[12, 15]. This similarities invite an interpretation that ascribes this interesting behavior to the properties shared by these compounds, namely, low carrier density and an equal number of electrons and holes (compensation). In contrast with that the metallic behavior remains at higher temperature even at high field in the WTe_2 [26] and $\beta\text{-Ag}_2\text{Te}$ [30, 31], the metal-insulator transition occurs at room temperature at above 2T field in the semimetal TaP, as shown in the inset in Fig.1(a), as well as TaAs[14].

The relative change of the MR at various temperatures as a function of magnetic field is plotted in Fig.2(c) and (d) by the typical definition of MR[34]: $\frac{\Delta\rho}{\rho(0)} = \left[\frac{\rho(H) - \rho(0)}{\rho(0)} \right] \times 100\%$, where $\rho(H)$ is the resis-

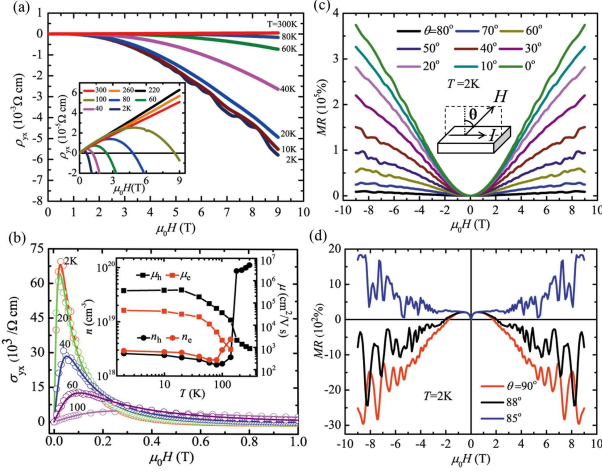


FIG. 3. (Color online) (a) The Hall resistivity versus magnetic field from 2 to 300K, strong SdH oscillation were observed below 10K. Inset: Hall resistivity for the higher temperatures and for lower temperatures in lower fields. (b) Hall conductivity σ_{yx} at five representative temperatures as a function of field. The solid lines are the fitting curves from the two-carrier model. Inset: The temperature dependence of the mobilities and carrier concentrations of the electrons and holes. (c) The MR versus magnetic field measured at 2K for various H alignment with respect to I . (d) The MR versus magnetic field measured at 2K for H near in parallel to I .

tivity measured at H for each given isotherm. At 2K, the MR reaches to $3.28 \times 10^5\%$ at 8T, two times larger than that in the recently reported compound WTe_2 at 2K in 8T although its RRR is 1-2 orders of magnitude less than that of the latter, and does not appear saturation in the highest field in our measurements. Remarkable, the MR at room temperature (300K) can reach to 176% at 8T, and increases almost linearly with field without any saturation, indicating that these WSMs can be used in the magnetic device in the future. It can be seen explicitly that there is a transition from quadratic MR at low magnetic fields to linear MR at high magnetic fields at a given temperature, as expected theoretically for the WSMs[35]. The relative MR of many metal and semimetals can be represented by the form, commonly referred to as Kohler's rule[34], $\Delta\rho/\rho(0)=F[H/\rho(0)]$, where $F(H)$ usually follows a power law. As shown in Fig.2(b), although all the MR data below 100K collapse onto the same curve, the MR does not follow a simple power law. And we found that the MR data above 100K does not collapse this curve, indicating that phonon scattering plays a role at higher temperatures. The following Hall resistivity and SdH oscillation analysis help to understand this complexity. Another, there are Shubnikov-de Haas (SdH) oscillations superimposing on the MR, which amplitude increases with decreasing temperature. Detailed analysis of the SdH data will be presented below.

Then, we discuss the charge carrier information about

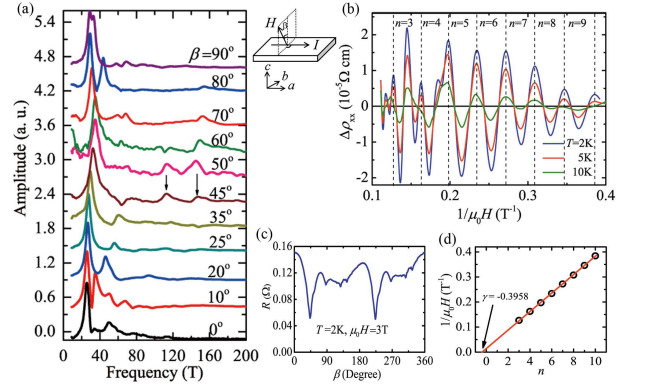


FIG. 4. (Color online) (a) The Fourier transformation for magnetoresistivity after subtracting the non-oscillation part, measured at 2K for various H alignment with respect to c axis, and keeping $H \perp I$. (b) $\Delta\rho_{xx}$ as a function of $1/\mu_0 H$ at 2K, 5K, and 10K, where $\Delta\rho_{xx}$ is the oscillation part in the magnetoresistivity ρ_{xx} after subtracting ρ_0 for $\beta=0$. (c) The angle dependence of resistance, $R_{xx}(\beta)$, measured at 2 K and 3 T. (d) Linear fitting of the Landau fan diagram for $F_1=25.6$ T, showing a non-trivial Berry's phase with strong offset of 0.3958.

TaP compound. Figure 3(a) shows the Hall resistivity as a function of magnetic field, $\rho_{yx}(H)$, measured at various temperatures. At higher temperatures (above 140K), the positive slope of $\rho_{yx}(H)$ indicates that the holes dominate the main transport processes. At lower temperatures (below 140K), even at the lowest temperature (2K) the slope of $\rho_{yx}(H)$ changes from a positive to a negative value with increasing field, as shown in the inset of Fig. 3(a), indicating the coexistence both electron and hole carrier charges. SdH oscillations superimposed on the $\rho_{yx}(H)$ at higher field below 10K is also obvious. As done in Ref.[14] for the TaAs compound, we fitted the Hall conductivity tensor calculated using $\sigma_{xy}=\rho_{yx}/(\rho_{xx}^2+\rho_{yx}^2)$ by adopting a two-carrier model[36], $\sigma_{xy}=[n_h\mu_h^2 \frac{1}{1+(\mu_h H)^2} - n_e\mu_e^2 \frac{1}{1+(\mu_e H)^2}]$. Where n_e (n_h) and μ_e (μ_h) denote the carrier concentrations and mobilities of the electrons (holes), respectively. Figure 3(b) presents the fitting for σ_{xy} data measured at five representative temperatures. It should be pointed out that the Hall conductivity above 180K is mainly from the hole band due to the thermal depopulation of hole-like pockets just above the Fermi level, thus the n_h and μ_h values above 180K were estimated by using a single band fitting. The obtained n_e (n_h) and μ_e (μ_h) values by fittings in whole temperature range are shown in the inset of Fig.3(b). At first, it is obvious that the n_e and n_h values at lower temperatures (below 100K) are almost the same, such as at 2K, $n_e=2.58 \times 10^{18}/\text{cm}^3$, $n_h=2.90 \times 10^{18}/\text{cm}^3$, indicating TaP is indeed a low carrier concentration, hole-electron compensated semimetal, which is in consistent with the discussions above about the extremely large MR. Notes that the n_h has an obvious increase at 140K with in-

creasing temperature. Secondly, at lower temperatures, the mobility of hole, μ_h , is one order of magnitude larger than μ_e , such as at 20K, $\mu_h=3.71\times 10^5 \text{ cm}^2/\text{V s}$, and $\mu_e=3.04\times 10^4 \text{ cm}^2/\text{V s}$, in contrast with that in other WSMs, such as TaAs[10, 14], NbAs[33] and NbP[12], in which usually $\mu_e>\mu_h$. Note that as increasing temperature, both μ_h and μ_e have an obvious decrease around 140K due to enhancement of phonon thermal scattering. The mobility of carriers in all the WSMs, such as TaAs, NbAs and NbP, verified recently, as well as TaP reported here, are comparable, but much higher than that in the conventional semimetals, such as WTe₂[26] and high purity Bi[22], graphite[28, 29]. This is related to the existence of Weyl fermion in these compounds.

In the WSM, due to the presence of chiral Weyl node pairs, unconventional negative MR induced by the Adler-Bell-Jackiw anomaly[38, 39] (also named as the chiral anomaly) would be expected when H is applied in parallel to the electric field E , *i.e.*, the current direction I . Thus, we measured the MR at 2K for the different angles, θ , denoted as in the inset of Fig.3(c), between H and I . As shown in Fig. 3(d), when $\theta=90^\circ$, *i.e.*, $H \parallel I$, the negative MR is indeed observed, reaches to near -3000% at 9T, and exhibits no signature of saturation even at the highest field in our measurements. This behavior is different with that in other WSMs, such as in TaAs[13], and NbP[15], in which MR changes soon from negative to positive value as H increases, and may be due to TaP having a larger distance of Weyl nodes in the momentum space[40]. Another, the MR curve has a small positive peak below 2T, which was also observed in Bi_{1-x}Sb_x[45], TaAs[13, 14] and NbP[15], and attributed to a weak anti-localization. It is obvious that the SdH oscillation superimposing onto the MR. If θ decreases to 88° , the unsaturated negative MR remains, but its value decreases. When $\theta \leq 85^\circ$, the MR becomes positive value and reaches the maximum value as $\theta = 0^\circ$, as shown in Fig.(c).

In order to get the information of the Fermi surface of TaP, we also measured the magnetoresistivity, $\rho_{xx}(H)$ (not shown here) for different angles β , between H and c axis, represented in the inset of Fig.4, and keeping $H \perp I$. Figure 4(c) shows the angle dependence of resistance measured at 2K and 3.0T. It is found that the resistance in magnetic field exhibits maximum at $\beta=0$, and reaches a minimum value at $\beta=45^\circ$, indicating the anisotropy of the Fermi surface topology. In fact, for all the angles, strong Shubnikov-de Haas (SdH) oscillations superimpose onto the $\rho_{xx}(H)$.

First, we discuss another interesting consequence due to the presence of chiral Weyl node pairs: a nontrivial Berry's phase (Φ_B) realizes in TaP, which is the characteristic feature of the charge carriers that have k -space cyclotron orbits enclosing a Dirac points.[41-44]. We use the expression[37]: $\rho_{xx}=\rho_0+\Delta\rho_{xx}=\rho_0[1+A(B,T)\cos 2\pi(F/B+\gamma)]$, to ana-

lyze the SdH oscillations in $\rho_{xx}(H)$, as $H \parallel c$ axis, *i.e.* $\beta=0^\circ$ in the Fig. 4. Here ρ_0 is the non-oscillatory part of the resistivity, $A(B,T)$ is the amplitude of SdH oscillations, $B=\mu_0H$ is the magnetic field, and γ is the Onsager phase, and $F=\frac{h}{2e\pi}A_F$ is the frequency of the oscillations, where A_F is the extremal cross-sectional area of the Fermi surface (FS) associated with the Landau level index n , e is the elementary charge, and $h=\frac{h}{2\pi}$, h is the Plank's constant. Figure 4(b) shows the $\Delta\rho_{xx}$ as a function of $1/\mu_0H$ at 2K, 5K, and 10K after subtracting ρ_0 . Obviously, there are two sets of oscillations, corresponding to two frequencies of $F_1=25.6 \text{ T}$, and $F_2=49.6 \text{ T}$, confirmed by its Fourier transformation ($\beta=0$) in Fig.4(a). According to Onsager relation, the extremal cross-sectional areas of the FS were estimated as $A_F=2.439\times 10^{-3} \text{ \AA}^2$, $4.725\times 10^{-3} \text{ \AA}^2$ corresponding to F_1 and F_2 , respectively, which are very small compared with the whole cross-sectional area of the first BZ[13]. Then we focus on the SdH oscillation with F_1 . To determine the Berry's phase of the carriers, we have plotted the Landau fan diagram, as shown in Fig. 4(d), linear fitting gives an Onsager phase of $\gamma=-0.3958$. The existence of a nontrivial Berry's phase with strong offset of 0.3958 confirms its Weyl fermions behavior. It has been predicted[10] by the *ab initio* calculations that there are 12 pairs of Weyl nodes in the Brillouin zone (BZ), the eight pairs locates at $k_z \sim \pm 0.6\pi/c'$ (named W1) where $c' = c/2$ and the other four pairs sit in the $k_z=0$ plane (W2). As H is applied along c axis, possible WSM electron pockets and hole pockets are quantized equivalently duo to the four-fold rotation symmetry of the Brillouin zone (BZ)[9]. So, we expect that the two major oscillation frequencies at $\beta=0^\circ$ are assigned to these two types Weyl nodes.

Second, we focus on the angle (β) dependence of the SdH oscillations frequency. As shown in Fig.4(a), with increasing β , F_1 peak at $\beta=0$ shifts to a little higher frequency then turns back, exhibiting a near isotropic behavior, as expected for W1 cones[9]. But for F_2 at $\beta=0$, corresponding to the anisotropic W2 nodes, it is difficult to give clear trend to change with angle β . Interestingly, there are another two peaks at $F'=112 \text{ T}$ and 146 T for $\beta=45^\circ$ and 50° curves, except for the major peak at 32.8T corresponding to W1 nodes. These high frequency peaks may originate from the other massive bands near FS, which seems to provide an explanation for the minimum of MR observed at $\beta=45^\circ$.

In summary, we have measured the longitudinal resistivity (ρ_{xx}) and Hall resistivity (ρ_{yx}) for TaP single crystal. It is found that at 2K its MR reaches to $3.28\times 10^5\%$, especially at 300K can reaches to 176% at 8T, and both do not appear saturation even at the highest field in our measurements. Hall resistivity measurements confirmed that TaP is indeed a low carrier concentration, hole-electron compensated semimetal, with the high mobility. Remarkably, as a magnetic field (H) is applied

in parallel to the electric field (E), the negative MR due to chiral anomaly is observed, reaches to near -3000% at 9T, and exhibits also no signature of saturation, which distinguishes with other WSMS. Based on the analysis Shubnikov-de Haas (SdH) oscillations superimposing on the MR, it is found that a nontrivial Berry's phase with strong offset of 0.3958 realizes in this compound, which confirms its Weyl fermions behavior.

This work is supported by the National Basic Research Program of China (973 Program) under grant No. 2015CB921004, 2012CB821404, and 2011CBA00103, the Nature Science Foundation of China (Grant No. 11374261, and 11204059) and Zhejiang Provincial Natural Science Foundation of China (Grant No. LQ12A04007), and the Fundamental Research Funds for the Central Universities of China.

During preparation of this manuscript the authors became aware of a related work by C. Shekhar et al. posted on arXiv [arXiv: 1506.06577].

* mhfang@zju.edu.cn

- [1] S. Murakami, *New J. Phys.* **9**,356(2007)
- [2] L. Balents, *Physics* **4**, 36(2011)
- [3] A. A. Burkov and L. Balents, *Phys. Rev. Lett.* **107**, 127205(2011)
- [4] A. A. Burkov, M. D. Hook and L. Balents, *Phys. Rev. B.* **84**, 235126(2011)
- [5] G. B. Halasz and L. Balents, *Phys. Rev. B.* **85**, 035103(2012)
- [6] X. Wan *et al.* *Phys. Rev. B.* **83**, 205101(2011)
- [7] G. Xu,*et al.* *Phys. Rev. Lett.* **107**, 186806(2011)
- [8] J. Liu *et al.* *Phys. Rev. B.* **90**, 155316(2014)
- [9] Hongming Weng, Chen Fang, Zhong Fang, B. Andrei Bernevig, and Xi Dai, *Phys. Rev. X.* **5**, 011029(2015)
- [10] Shin-Ming Huang, *et al.*, arXiv: 1501.00755
- [11] B. Q. Lv *et al.*, arXiv:1503.09188
- [12] Chandra Shekhar *et al.*, arXiv:1502.04361
- [13] Xiaochun Huang *et al.*, arXiv:1502.01304
- [14] Chenglong Zhang *et al.*, arXiv:1502.00251
- [15] Zhen Wang *et al.*, arXiv:1506.02282
- [16] J. E. Lenz, *Proc. IEEE* **78** 973(1990)
- [17] Y. Moritomo, A. Asamitsu, H. Kuwahara and Y. Tokura, *Nature* **380** 141(1996)
- [18] J. Daughton, *J. Magn. Magn. Mater.* **192** 334(1999)
- [19] W. F. Egelhoff *et al.*, *J. Appl. Phys.* **78** 273(1995)
- [20] A. P. Ramirez, R. J. Cava and J. Krajewski, *Nature* **386** 156(1997)
- [21] S. Jin, M. McCormack, T. H. Tiefel and R. Ramesh, *J. Appl. Phys.* **76** 6929(1994)
- [22] F. Y. Yang *et al.* *Science* **284** 1335(1999)
- [23] R. Xu, *et al.*, *Nature* **390** 57(1997)
- [24] S. Ishiwata *et al.* *Nature Mater.* **12** 512(2013)
- [25] S. A. Solin, T. Thio, D. R. Hines, and J. J. Heremans, *Science* **289** 1530(2000)
- [26] Mazhar N. Ali *et al.*, *Nature* **514**, 205(2014)
- [27] Xiaojun Yang *et al.*, arXiv:1503.07571(2015)
- [28] Y. Kopelevich *et al.* *Phys. Solid State* **41**, 1959(1999)
- [29] Y. Kopelevich *et al.*, *Phys. Rev. Lett.* **90**, 156402(2003)
- [30] R. Xu *et al.*, *Nature (London)* **390**, 57(1997)
- [31] W. Zhang *et al.*, *Phys. Rev. Lett.* **106**, 156808(2011)
- [32] L. P. He *et al.*, *Phys. Rev. Lett.* **113**, 246402(2014)
- [33] N. J. Ghimire *et al.*, arXiv: 1503.07571
- [34] A. B. Pippard, *Magneto-resistance in Metals*(Cambridge University Press, Cambridge, 1989)
- [35] N. Ramakrishnan, M. Milletari, and Shaffique Adam, arXiv: 1501.03815
- [36] Colin M. Hurd, *The Hall effect in metals and alloys*(Cambridge University Press, Cambridge, 1972)
- [37] H. Murakawa *et al.*, *Science* **342**, 1490(2013)
- [38] S. Adler, *Phys. Rev.* **177**, 2426(1969)
- [39] J. S. Bell and R. Jackiw, *Nuovo Cimento A* **60**, 4(1969)
- [40] N. Xu *et al.*, arXiv: 1507.03983
- [41] G. P. Mikitik, Yu V. Sharlai, *Phys. Rev. Lett.* **82**, 2147(1999)
- [42] G. P. Mikitik, Yu V. Sharlai, *Phys. Rev. Lett.* **93**, 106403(2004)
- [43] K. S. Novoselov *et al.*, *Nature* **438**, 197(2005)
- [44] Y. Zhang, Y. W. Tan, H. L. Stormer, P. Kim, *Nature* **438**, 201(2005)
- [45] H. J. Kim *et al.*, *Phys. Rev. Lett.* **111**, 246603(2013)